Cell, Vol. 116, 711–723, March 5, 2004, Copyright ©2004 by Cell Press

Crystal Structures of a Formin Homology-2 Domain Reveal a Tethered Dimer Architecture

Yingwu Xu,[1,2] James B. Moseley,[3] Isabelle Sagot,[4] Florence Poy,[1] David Pellman,[4,*] Bruce L. Goode,[3] and Michael J. Eck[1,2,*]
[1]Department of Cancer Biology
Dana-Farber Cancer Institute
44 Binney Street
Boston, Massachusetts 02115
[2]Department of Biological Chemistry and Molecular Pharmacology
Harvard Medical School
Boston, Massachusetts 02115
[3]Department of Biology and
The Rosenstiel Basic Medical Sciences Research Center
Brandeis University
415 South Street
Waltham, Massachusetts 02454
[4]Departments of Pediatric Oncology
The Dana-Farber Cancer Institute and Pediatric Hematology
The Children's Hospital
Harvard Medical School
44 Binney Street
Boston, Massachusetts 02115

Summary

Formin proteins participate in a wide range of cytoskeletal processes in all eukaryotes. The defining feature of formins is a highly conserved ~400 residue region, the Formin Homology-2 (FH2) domain, which has recently been found to nucleate actin filaments. Here we report crystal structures of the *S. cerevesiae* Bni1p FH2 domain. The mostly α-helical FH2 domain forms a unique "tethered dimer" in which two elongated actin binding heads are tied together at either end by an unusual lasso and linker structure. Biochemical and crystallographic observations indicate that the dimer is stable but flexible, with flexibility between the two halves of the dimer conferred by the linker segments. Although each half of the dimer is competent to interact with filament ends, the intact dimer is required for actin nucleation and processive capping. The tethered dimer architecture may allow formins to stair-step on the barbed end of an elongating nascent filament.

Introduction

Different actin nucleators have recently been linked to the assembly of actin structures with distinct architectures (Evangelista et al., 2002, 2003; Feierbach and Chang, 2001; Pruyne et al., 2002; Sagot et al., 2002a, 2002b). The Arp2/3 complex nucleates branched filaments whereas formins nucleate short linear filaments. In budding yeast, the Arp2/3 complex is specifically required for the assembly of actin patches, which are involved in endocytosis (Kaksonen et al., 2003; Moreau et al., 1996; Winter et al., 1997). By contrast, yeast formins are specifically required for the assembly of actin cables, linear structures that serve as tracks for the directional transport of materials necessary for polarized morphogenesis (Evangelista et al., 2002; Feierbach and Chang, 2001; Sagot et al., 2002a). In mammalian cells, the Arp2/3 complex is required for the assembly of structures such as lamellipodia that contain networks of branched actin filaments (Pollard et al., 2000). Mammalian formins have been linked to the assembly of linear structures such as actin stress fibers (Tominaga et al., 2000; Watanabe et al., 1999). In all eukaryotic cells examined, formins are required for cytokinesis and are essential for the assembly of the actin contractile ring, a structure thought to contain antiparallel arrays of linear actin filaments (Evangelista et al., 2003; Wallar and Alberts, 2003). In addition to their role in actin assembly, formins are also required to orient some actin cytoskeletal structures to polarized membrane sites (Evangelista et al., 2002; Sagot et al., 2002a).

Formins are large, multidomain proteins that interact with diverse signaling molecules and cytoskeletal proteins (Castrillon and Wasserman, 1994; Evangelista et al., 2002, 2003; Feierbach and Chang, 2001; Sagot et al., 2002a; Tominaga et al., 2000; Wallar and Alberts, 2003; Watanabe et al., 1999). The "Diaphanous-related" formins (DRFs) are effectors for Rho-family GTPases (Evangelista et al., 1997; Kohno et al., 1996; Watanabe et al., 1997) and contain an N-terminal GTPase binding domain (GBD), an FH3 region that may be important for localization (Petersen et al., 1998), a proline-rich FH1 domain, and a characteristic C-terminal FH2 domain (Figure 1A). The binding of Rho-GTP is thought to activate DRFs by relieving an autoinhibitory interaction between the GBD and a short segment at the C-terminal end of the FH2 domain, the Diaphanous autoinhibitory domain or DAD (Alberts, 2001; Li and Higgs, 2003; Watanabe et al., 1999). In vitro, the FH2 domain of the budding yeast formin Bni1p promotes the nucleation of actin filaments (Pring et al., 2003; Pruyne et al., 2002; Sagot et al., 2002b). The actin monomer binding protein profilin further stimulates actin assembly induced by Bni1 constructs containing both the FH1 and FH2 domains (Sagot et al., 2002b; Moseley et al., 2003). Profilin binds to the proline-rich FH1 domain (Evangelista et al., 1997; Imamura et al., 1997), which is positioned immediately N-terminal to the FH2 domain. The Bni1 FH2 domain forms a stable dimer, and mutations that disrupt dimerization abolish FH2 domain activity (Moseley et al., 2003). Dimerization might be relevant to the nucleation mechanism because kinetic studies suggest that Bni1 may induce filament formation by stabilizing an actin dimer (Pring et al., 2003). Although the size of full-length formin complexes has not been determined, hydrodynamic studies of formin fragments suggest that formins form oligomers (Li and Higgs, 2003; Zigmond et al., 2003).

*Correspondence: eck@red.dfci.harvard.edu (M.J.E.), David_Pellman@dfci.harvard.edu (D.P.)

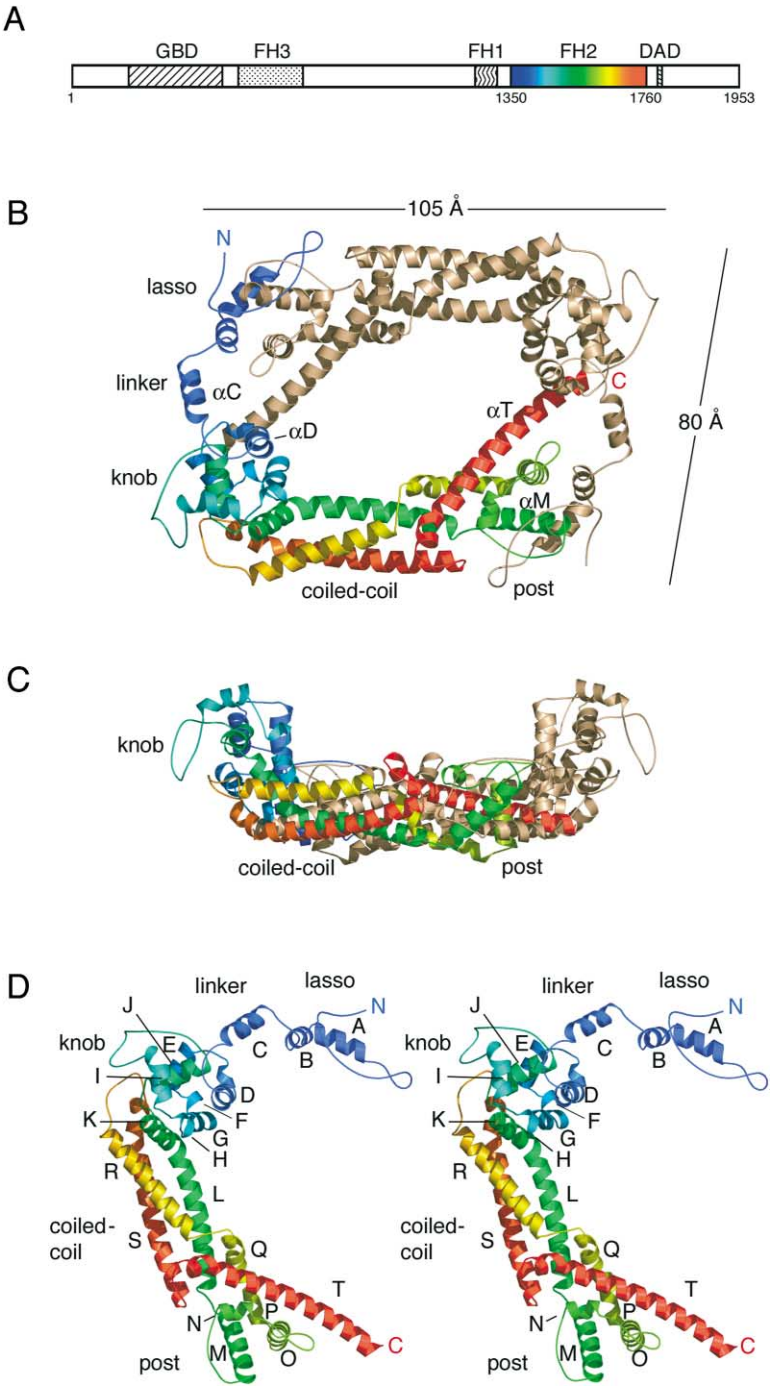

Figure 1. Three-Dimensional Structure of the FH2 Domain Dimmer

(A) Domain organization of Bni1p.

(B) Ribbon diagram showing the overall architecture of the FH2 dimer. One molecule is colored using the visible spectrum (from blue at the N terminus to red at the C terminus), the second molecule is colored tan. The lasso, linker, knob, coiled-coil, and post subdomains are labeled, and the approximate dimensions of the dimer are indicated. The N and C termini and selected α helices of one molecule are labeled. Note the manner in which the lasso region of each molecule encircles a portion of the post subdomain of the other molecule in the dimer.

(C) Side view of the FH2 domain dimer.

(D) Stereodiagram depicting the fold of the FH2 domain. Helices are labeled alphabetically.

Formins appear to promote actin assembly by a unique molecular mechanism. The Arp2/3 complex caps the slow growing pointed end of actin filaments and promotes assembly from the fast growing barbed end (Pollard et al., 2000). The two actin-related proteins in the Arp2/3 complex are hypothesized to contribute directly to the nucleus from which new filaments are extended (Robinson et al., 2001). By contrast, the FH2 domains of Bni1 and mDia bind the barbed ends of actin filaments (Li and Higgs, 2003; Moseley et al., 2003; Pruyne et al., 2002) but nonetheless promote barbed end actin assembly (Li and Higgs, 2003; Moseley et al., 2003; Pruyne et al., 2002; Sagot et al., 2002b; Zigmond et al., 2003). Initial evidence suggested that formins have a high affinity interaction with the barbed end (Li and Higgs, 2003; Pring et al., 2003; Pruyne et al., 2002); this is further supported by the observation that nanomolar concentrations of Bni1 or mDia protect the growing barbed ends of filaments from high concentrations of capping proteins (Zigmond et al., 2003; Moseley et al., 2003). The degree of barbed end capping differs for different formin FH2 domains (Kovar et al., 2003; Li and Higgs, 2003; Pring et al., 2003; Pruyne et al., 2002; Zigmond et al., 2003). At one extreme is the FH2 domain

of Cdc12p, a formin required for cytokinesis in fission yeast, which on its own completely caps the barbed end of actin filaments and only allows barbed end elongation in the presence of profilin (Kovar et al., 2003). At the other extreme is the mDia FH2 domain that has minimal barbed end capping activity (Li and Higgs, 2003). Further, in the presence of profilin, cdc12 prevents the annealing of actin filaments (Kovar et al., 2003). Together, these results suggest that formins persistently associate with the barbed end during filament elongation forming a processive cap.

To better understand the mechanism by which formins promote actin assembly, we determined the crystal structure of the Bni1p FH2 domain. The structure reveals a tethered dimer architecture consisting of two elongated actin binding heads connected at either end by apparently flexible linker segments contributed by each subunit. Proteolytic cleavage within the linkers yields "hemidimers," which block the barbed end of actin filaments but lack the normal nucleation and processive capping activities of the intact dimer.

Results and Discussion

Structure of the FH2 Domain

We prepared over two dozen FH2 expression constructs with different N- and C-terminal boundaries for crystallization trials. The protein encoded by construct "Z" (residues 1348–1766 of Bni1p) was functional and yielded crystals suitable for structure determination in the presence of p-chloromercuribenzene sulfonic acid (PCMBS, see Experimental Procedures). Analysis of Z and similar fragments by gel filtration and analytical ultracentrifugation revealed that the FH2 domain is a stable dimer in solution (Moseley et al., 2003). The structure was determined by MAD phasing methods (Table 1). The final model contains residues 1350–1760 of Bni1p and has been refined to an R value of 20.7% (R free = 25.1%) using anisotropic data extending to 2.5 Å along the hexagonal axis and to 3.1 Å in the perpendicular plane.

When viewed from the top, the FH2 dimer forms a closed ring in the shape of a parallelogram (Figure 1B). The FH2 domain can be subdivided into five subdomains with somewhat arbitrary boundaries. These include an N-terminal "lasso," a 17 residue "linker" segment, a globular "knob" subdomain, a coiled-coil region, and a carboxy-terminal "post" subdomain (Figure 1). In the FH2 domain dimer, the two subunits interact in a head-to-tail orientation. Dimerization is mediated by the unusual lasso structure; in a reciprocal manner, the lasso in each subunit encircles a protuberance on the post subdomain of the other molecule. The knob, coiled-coil, and post of one subunit, together with the lasso of the dimer-related subunit, share a continuous hydrophobic core and comprise a single structural unit that we refer to hereafter as a "hemidimer." The two relatively rigid hemidimers are leashed together by the linker segment of each molecule to form the tethered dimer architecture. The FH2 domain fold appears to be intrinsically dimeric, as the residues in the lasso/post interface are highly conserved (Figure 2). The dimer is perfectly symmetric in the crystal, as the two subunits are related by a crystallographic 2-fold axis, but the linker region is likely to afford considerable flexibility between the two halves of the dimer in solution (see below). The two knob regions of the dimer extend prominently above the plane of the parallelogram, giving the molecule a boat-shaped appearance when viewed from the side (Figure 1C).

The FH2 domain fold is almost entirely α helical (Figures 1D and 2). The first 51 residues, including helices αA and αB, form the lasso. Immediately following the lasso, helix αC and flanking sequences constitute the linker segment (residues 1401 to 1417). The knob region follows in primary sequence and is composed of eight α helices that form a compact globular subdomain. Amino acid substitutions that are encoded by two temperature-sensitive *BNI1* alleles, Asp1511Asn (Evangelista et al., 2002) and Arg1528Ala (Sagot et al., 2002a), are likely to destabilize the knob region as they disrupt important buried electrostatic interactions. The knob subdomain is tightly integrated with the coiled-coil region via helix αK and the RS loop (loops are named for the helices that they connect). From the knob, the polypeptide chain passes through the coiled-coil (αL) and then forms the bulk of the post region (including helices αM through αQ). Helices αR and αS cross to and from the knob subdomain, respectively, and contribute the second and third helices to the triple-helical coiled-coil region. Finally, the long and kinked C-terminal helix αT completes the post subdomain. Searches of the DALI and VAST structure databases reveal no significant similarity between the FH2 domain and other proteins of known structure (aside from the superficial similarity of the coiled-coil region to other coiled-coil proteins).

The Unique Lasso/Post Dimer Interface

The observed head-to-tail mode of dimerization yields two identical dimer interfaces—the lasso of each subunit encircles the post region of the other subunit in the dimer. The lasso region winds about 1 1/3 turns around helix αM and the MN loop in the dimer-related subunit (Figure 3A). The first 28 residues of the lasso lack regular secondary structure, and two tryptophan residues in this region insert into hydrophobic pockets in the post (Figure 3B). These tryptophan residues, as well as glycines residues found in each of the receiving pockets (glycines 1576 and 1588), are among the most highly conserved residues in the FH2 fold (Figure 2). This portion of the lasso also forms an extensive network of hydrogen bonds with the post region (Figure 3C). The "G-N-Y/F-M-N" sequence motif that originally defined the FH2 domain lies within helix αM in the post region and all of the residues in this motif participate in dimerization (residues 1576–1580 in Bni1p). On the opposite side of the post, helices αA and αB in the lasso pack into shallow hydrophobic grooves (Figure 3D). Interestingly, the loop portion of the lasso "closes" upon itself with two backbone-to-backbone hydrogen bonds (flanking Leu1358 and Ala1400) and with a hydrogen bond between the sidechain of Glu 1396 and the mainchain amide of His1355 (not shown).

The extensive contacts in the lasso/post interface would be expected to give rise to a very stable dimer. The surface area of this interaction is 1895 Å^2 (in each lasso/post interface), thus a total surface area of approximately 7580 Å^2 is buried upon dimerization. Our pre-

Table 1. X-ray Data, Phasing, and Refinement Statistics

Data Collection Statistics					
Crystal	Z, PCMBS-1	Z, PCMBS-2	Z, SeMet+PCMBS		Δ Z
Wavelength (Å)	0.916	0.936	1.0072	1.0093	0.978
Resolution (Å)	2.5 (2.6–2.5)	2.8 (2.9–2.8)	3.0 (3.11–3.0)	3.2	3.3
Number of reflections					
Total	154,481	122,568	131,054	107,881	50,090
Unique	49,995	34,466	30,600	24,417	22,747
Completeness (%)[a]	94.5(90.0)	90.4(89.3)	99.3(96.1)	97.9(94.0)	82(61)
I/σ	12.9(1.7)	9.0(2.5)	16.4(1.9)	12.8(2.2)	12.5(4.5)
R_{merge} (%)[b]	8.7(45.8)	(8.3)(41.3)	9.7(37.4)	9.8(30.8)	5.8(14.3)
Phasing Statistics					
Mercury sites	2	2	2	2	
SeMet sites			7	7	
Cullis_R_anomalous[c]	0.87	0.85	0.86	0.94	
Figure of merit[3]	0.29/0.85 (MLPHARE/CNS)				
Refinement Statistics					
Resolution (Å)	30–2.5				30-3.3
Reflections[d]	34,619				22,588
Number of protein atoms	3,335				6669
Number of waters	33				0
Number of other atoms[e]	12				0
R_{cryst}/R_{free} (%)[f]	20.7/25.1				23.4/28.8
Average B-factor	70.7				67.3
Bond lengths (Å)	0.007				0.008
Bond angles (°)	1.21				1.37

We also collected a three-wavelength selenomethionine MAD experiment, but these data are not shown here as they did not significantly improve phasing.

[a] Values in parentheses correspond to highest resolution shell.

[b] $R_{merge} = \Sigma_{hkl}|I_{hkl} - <I_{hkl}>|/\Sigma_{hkl} I_{hkl}$, where I_{hkl} is the measured intensity of the reflections with indices hkl.

[c] To the resolution 3.3 Å. Cullis_R_anomalous and figure of merit were calculated for the acentric reflections in MLPHARE. The phase information was then imported to CNS for density improvement.

[d] An ellipsoid reflection cutoff has been used to filter the data (see Supplemental Experimental Procedures online).

[e] Includes one PCMBS molecule and one additional mercury atom.

[f] R values were calculated with data $F > 0\sigma$.

vious analysis of the Bni1p FH2 domain by analytical ultracentrifugation showed that the sedimentation equilibrium data were best fit by a single molecular species of ~93,000 g/mol as expected for a stable dimer. In order to further assess the stability of the dimer, we mixed FH2 domain homodimers of differing electrophoretic mobilities and analyzed the mixture by native gel electrophoresis. Significant dissociation and rebinding would be expected to lead to formation of a heterodimeric species of intermediate electrophoretic mobility. No such band appears over the course of 11 days (Supplemental Figure S2 at http://www.cell.com/cgi/content/full/116/5/711/DC1). We conclude that the FH2 dimer is stable and has an extremely slow off rate. Additionally, the dimeric form of the FH2 domain appears to be required for actin nucleation. We have previously demonstrated that alanine substitutions of the two tryptophan residues in the lasso destabilizes the dimer and abrogates actin assembly and that truncation of residues 1348–1407 of construct Z (corresponding to the lasso and part of the linker) yields an inactive, monomeric protein (Moseley et al., 2003). These observations, together with the high degree of conservation of the dimer interface, indicate that the reciprocal lasso/post mode of dimerization we observe here is required for formin function and is likely to pertain to most, if not all formin proteins.

Identification of Likely Sites of Actin Binding

To define possible sites of interaction with actin, we studied the conservation of amino acid sidechains on the surface of the FH2 domain. Highly conserved residues that are solvent exposed and not required for the structural integrity of the domain are likely to play important functional roles. We compared the sequences of the 56 FH2 domains aligned in the Pfam database (Bateman et al., 2002) of protein domains and mapped the rate of evolutionary variation (Pupko et al., 2002) of each residue onto the surface of the Bni1 FH2 domain (Figures 4A and 4B). In contrast to the relatively featureless underside of the domain, the top surface reveals two clusters of highly conserved residues on each molecule in the dimer. One conserved surface patch is on the knob subdomain and is formed by the exposed surface of helix αD. In particular, isoleucine 1431 is highly conserved, even though it is completely solvent exposed. The second conserved patch lies at the opposite end of the hemidimer and is formed by residues in the post subdomain together with the lasso of the other subunit. This second surface is irregular and includes many of the residues that stabilize the dimer. However, the sidechains of some of the conserved residues are not important for dimerization and may be conserved because they are required for actin binding per se. For example, Lysine 1601 in the post region is very highly conserved

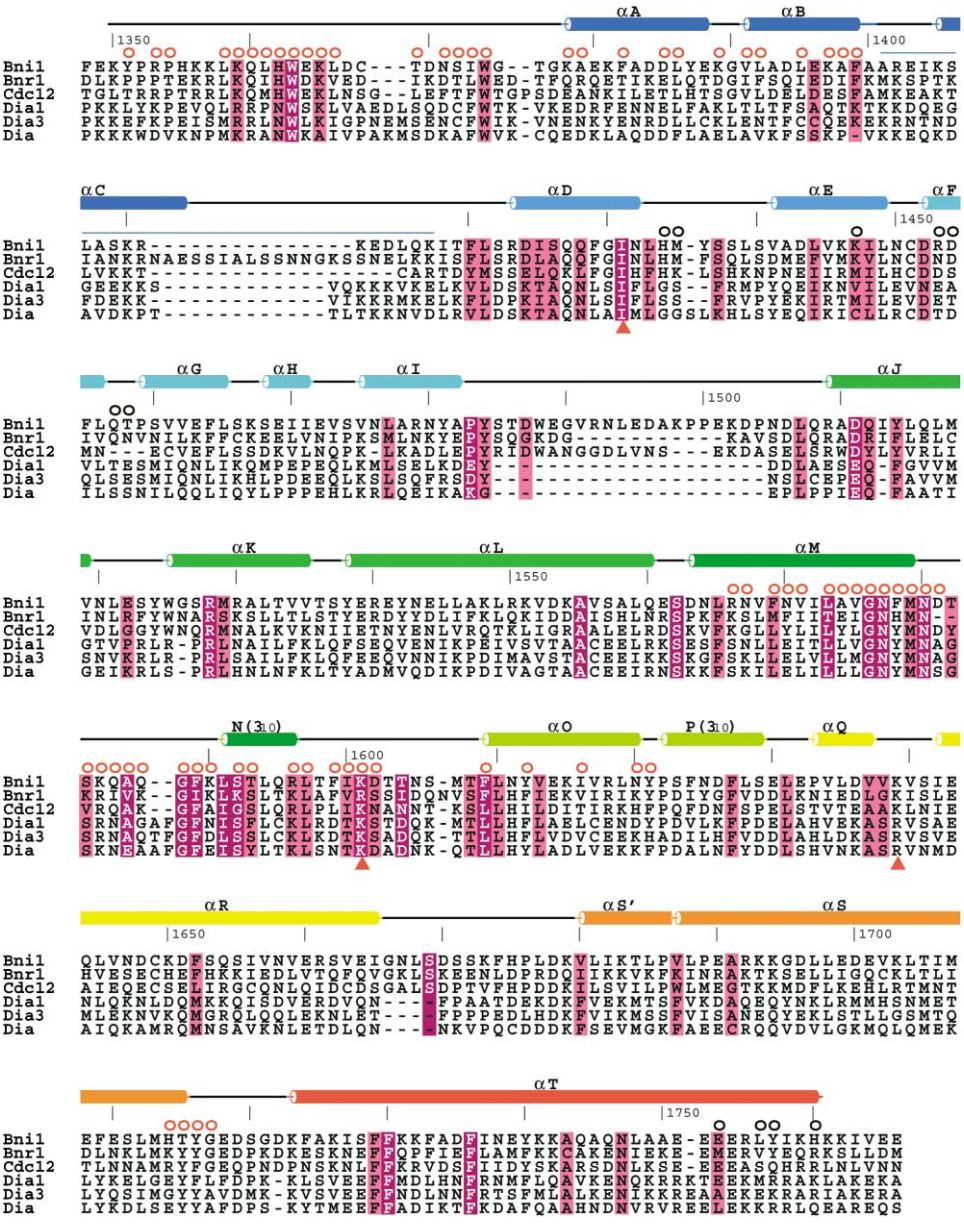

Figure 2. Sequence Alignment and Secondary Structure of the FH2 Domain

Aligned sequences are from *S. cerevisiae* Bni1p and Bnr1p, *S. pombe* Cdc12p, human diaphanous protein 1 (Dia1), mouse Dia3, and the *Drosophila* diaphanous (Dia) proteins. Secondary structure elements are shown above the sequences, with cylinders representing helices and thin lines indicating nonhelical structured regions. Helices are colored as in Figure 1; the structure is all α helical except for helices N and P, which have a 3_{10} pitch. Bni1p residues are numbered every 50 amino acids. Residues in the lasso/post dimer interface are indicated by red circles, those in the interface between the knob and helix αT of the second molecule are indicated by black circles. The light blue line indicates the linker. Red triangles indicate locations of point mutations studied here. Based on rate of evolutionary variation, highly conserved residues are marked with magenta shading and the most highly conserved are shown in white text on dark magenta (see also Figure 4). Note that many of the most highly conserved residues in the FH2 domain are found in the lasso/post dimer interface, indicating that the dimeric nature of the FH2 domain is conserved throughout phylogeny and among diverse formin proteins.

but participates in dimer formation only through its main-chain atoms. Structurally, this position should accommodate any charged or polar residue.

To assess the importance of these two conserved surfaces in actin nucleation, we introduced point mutations at positions 1431 and 1601 and tested the activity of the mutant and wild-type FH2 domains in an actin assembly assay (Figure 4C). Substitution of Ile1431 with alanine or of Lys1601 with aspartic acid completely abolished the actin nucleating activity of the FH2 domain. In addition, these substitutions eliminate the ability of the FH2 domain to slow elongation and to protect the barbed end from heterodimeric capping protein (Supplemental Figure S3 on the *Cell* website). Mutation of several conserved residues remote from these patches had no effect, or only a modest effect, on actin assembly

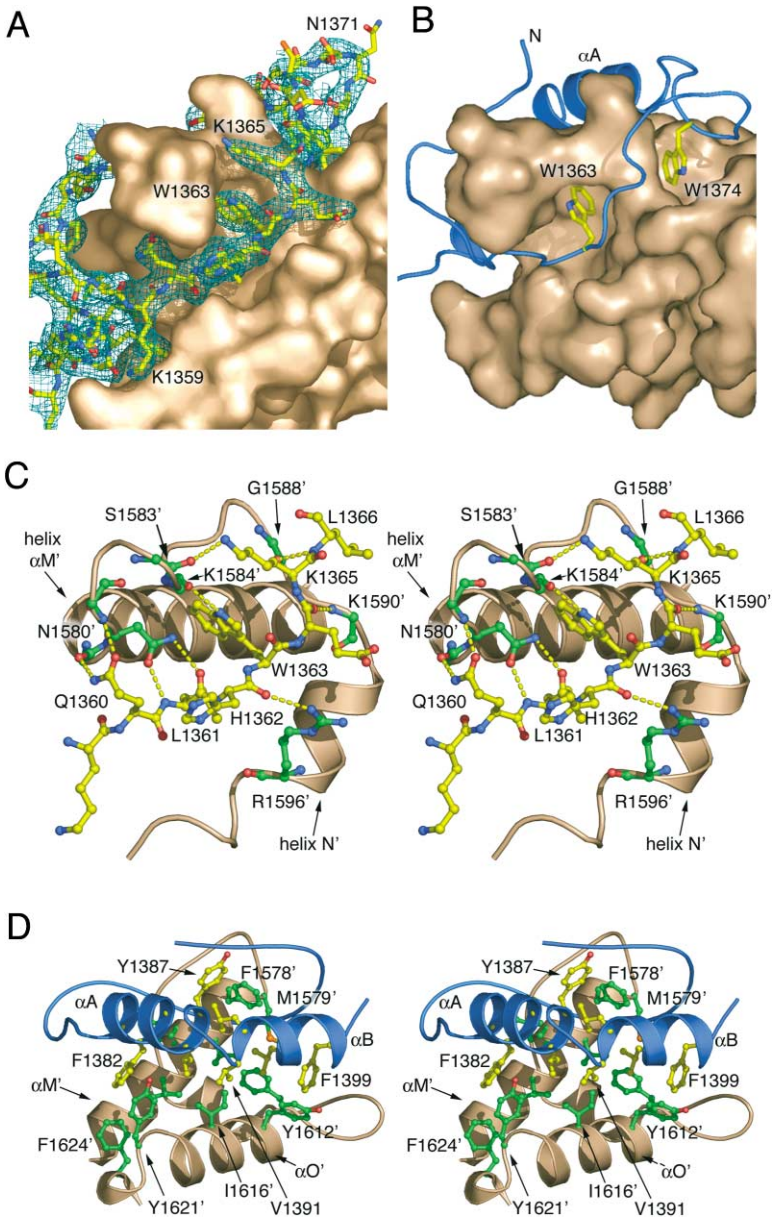

Figure 3. Extensive Interactions in the Lasso/Post Interface Stabilize the FH2 Dimer

(A) The 2Fo-Fc electron density map (cyan mesh) is contoured at 1.2σ in the region of the lasso (yellow stick model). The post region of the dimer-related molecule is shown as a tan surface.

(B) Conserved tryptophan residues 1363 and 1374 insert into hydrophobic pockets in the post.

(C and D) Stereo views of the lasso/post dimer interface, emphasizing some of the extensive hydrogen bond and hydrophobic interactions that stabilize the dimer. The prime symbol (′) denotes residues in the dimer-related molecule. (C) Residues 1360–1366 in the lasso are shown as a stick model (yellow) with the interacting region of the second molecule shown as a tan ribbon with green sidechains. Hydrogen bonds are indicated by dotted yellow lines. (D) On the opposite side of the lasso/post interface, helices αA and αB in the lasso (blue ribbon with yellow sidechains) pack with helices αM′ and αO′ in the post (tan and green). Note the extensive hydrophobic core stabilizing the interaction.

(Figure 4C). We conclude that the conserved surface patches on the upper surface of each hemidimer (marked by Ile1431 and Lys1601) are crucial for actin nucleation and barbed end capping, and that it is most likely this surface that contacts the actin filament.

The FH2 Domain Is a Flexible Dimer

What significance should be attached to the specific orientation of the two halves of the dimer that we observe in the crystal structure of construct Z? Because molecules must pack together to form a stable crystal lattice, it is important to ask whether the contacts that stabilize the particular 2-fold symmetric orientation are functionally relevant, or alternatively, whether they arise solely from crystal packing. As described above, the highly conserved lasso/post interface drives dimerization in solution and is clearly required for FH2 domain function. However, the structure suggests that in solution the two sides of the dimmer—the hemidimers—are very unlikely to be constrained in the 2-fold symmetric orientation we observe in the crystal structure. Rather, they are likely to be mobile with respect to one another, restrained only by the apparently flexible 17 residue linker segments that join them. A number of experimental observations support this interpretation. In the crystal structure, the linker segment is poorly ordered, with an overall temperature factor of over 100 Å^2 (as compared with 71 Å^2 for the structure as a whole). Limited proteolysis experiments reveal that the linker is readily cleaved by both chymotrypsin and trypsin within helix αC (Supplemental Figure S4A on the *Cell* website). These sites would not be expected to be accessible to proteases if maintained in a stable helical conformation. Additionally, the linker region bears hallmarks of a disordered poly-

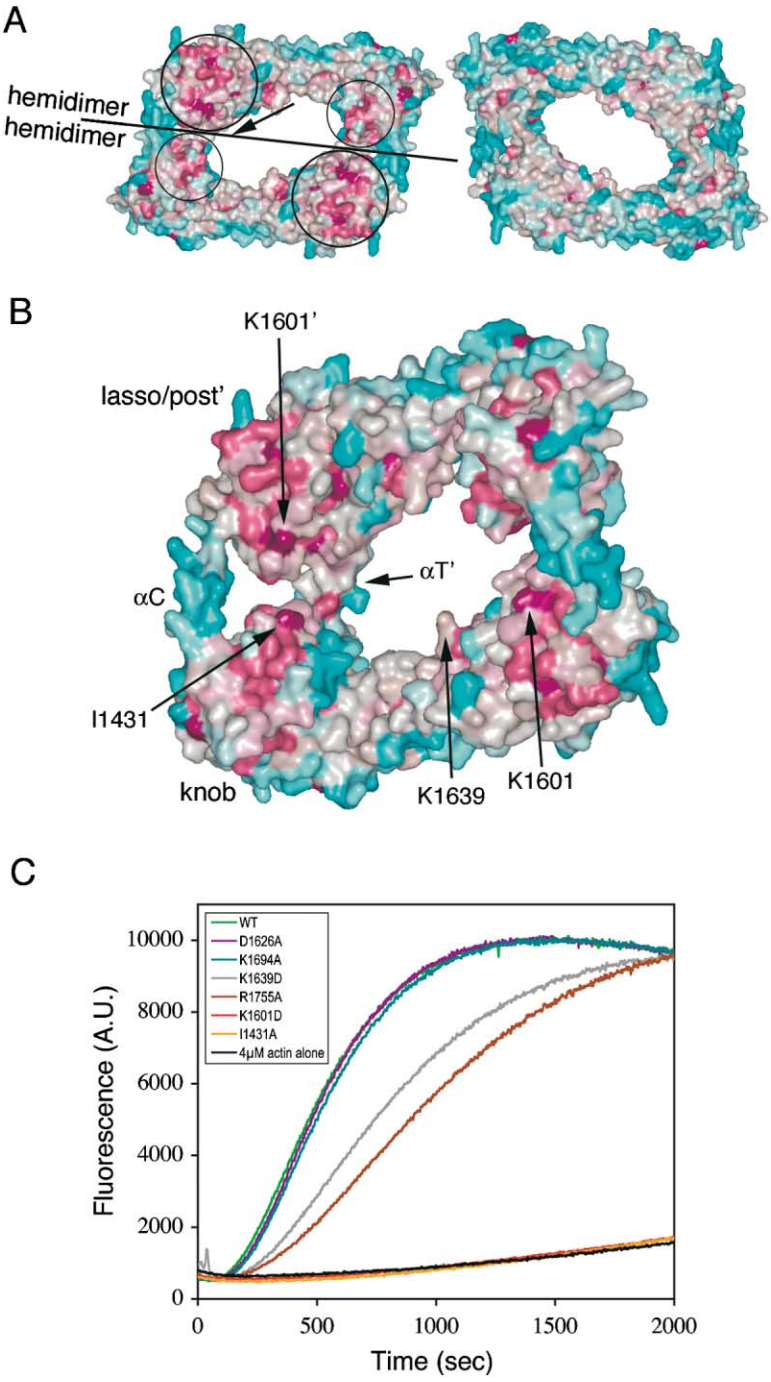

Figure 4. Conserved Surfaces on the Knob and Lasso/Post Regions Are Required for Actin Nucleation

(A) Views of the top (left panel) and bottom (right panel) surfaces of the FH2 dimer, colored by sequence conservation. The rate of evolutionary variation among 56 FH2 domain sequences (Pupko et al., 2002) was used to shade the molecular surface of the Bni1 FH2 domain in a gradient from dark teal (most variable residues) to white to dark magenta (most highly conserved residues). The upper surface of each hemidimer (left) reveals two conserved surface patches (circled). The arrow indicates the angle of view in (B), and the horizontal line indicates the approximate division of the dimer into hemidimers.

(B) Oblique view of the FH2 surface, highlighting the conserved surfaces around Ile1431 and Lys1601 that may represent sites of interaction with actin. As shown in (C), point mutations in either of these residues eliminate actin nucleation.

(C) Actin polymerization assay with wild-type and mutant Bni1p FH2 domain proteins. Four micromoles actin was assembled in the presence of 1 μM wild-type or mutant FH2 construct Z as indicated. The wild-type FH2 domain (green curve) reduces the lag phase and accelerates assembly as expected for an actin nucleator, but the I1431A and K1601D mutants have no effect. In contrast, "control" mutations in residues remote from the proposed actin binding surfaces (K1639D) or on the poorly conserved underside of the FH2 domain (D1629A, K1694A, and R1755A) have wild-type or near wild-type activity.

peptide segment; it is rich in charged and hydrophilic residues and its sequence and length are divergent among FH2 domains (Figures 2 and 4B). Apart from the linker, the only contact that might constrain the hemidimers is formed by helix αT. The C-terminal turns of αT make a glancing contact with the knob region of the neighboring subunit, but the residues involved are not conserved (Figures 2 and 5A).

To directly determine whether the observed 2-fold symmetric arrangement of subunits in the formin dimer is required for function, we tested the actin assembly activity of formin constructs in which the αT/knob contact and the linker segment were disrupted by deletions (constructs P and ΔZ, respectively). In construct P, the ten C-terminal residues of αT are not present (construct P includes residues 1348 to 1750 of Bni1p and was referred to as FH2(core) in Moseley et al., 2003). ΔZ is a variant of construct Z in which the linker is shortened by four amino acids. While construct ΔZ retains approximately half the activity of the wild-type protein, construct P is more that 2-fold more active than Z (Figure 6). The reason for the differences in activity among these constructs is unclear, but notably, both constructs retain activity in spite of deletions that perturb the contacts

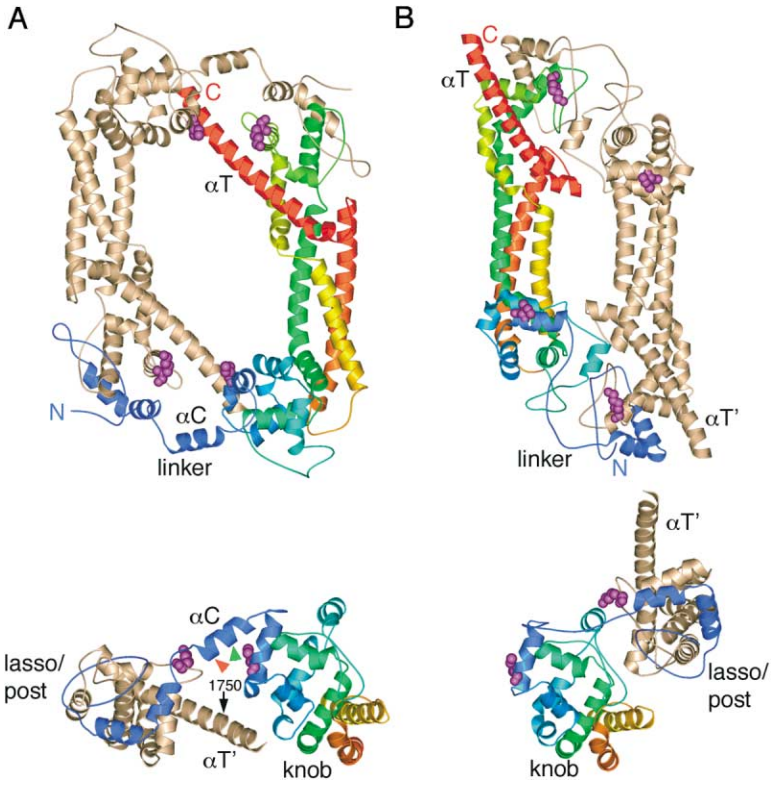

Figure 5. Comparison of the Two Bni1p FH2 Domain Crystal Structures

The structure of construct Z (A) is shown beside that of ΔZ (B). For both, an "end" view is shown below the top view. The subunits are colored as in Figure 1, and residues Ile1431 (on the knob) and Lys1601 (on the post) are shown in purple to mark the putative actin binding sites. Note that in the ΔZ structure, the tan subunit packs on the opposite side of the rainbow-colored subunit. In the end views, the rainbow subunits are presented in an identical orientation to highlight the difference in the position of the tan subunit. In the end view in (A), the chymotrypsin and trypsin cleavage sites in the linker segment are marked with red and blue arrows, respectively, and the C-terminal extent of construct P is indicated (residue 1750).

that define the orientation of the hemidimers. Furthermore, a Bni1p construct that terminates at residue 1750 is able to complement a temperature-sensitive allele of *BNI1* in vivo (Sagot et al., 2002b). These experiments show that the two structural features that define the relative orientation of the hemidimers in the crystal structure, αT/knob contact and the precise conformation of the linker, are both dispensable for actin assembly.

Finally, we sought to obtain additional crystal forms that might reveal different relative orientations of the hemidimers. We reasoned that observing an alternative relative orientation would directly prove the flexibility of the FH2 dimer. We were unable to obtain a second crystal form with constructs Z or P, but we were able to crystallize and determine the structure of ΔZ. The packing of the ΔZ crystals is unrelated to that of the Z crystals (Supplemental Figure S5 online). As expected, the ΔZ crystals reveal an essentially identical hemidimer structure, including the lasso/post interface (the Z and ΔZ hemidimers superimpose with an RMSD of 0.89 Å for α-carbon atoms). In contrast, the relative orientation of the hemidimers is markedly different in the two structures (Figure 5). The two subunits are again lashed together head-to-tail by the lasso and are related by crystallographic 2-fold symmetry, but they interact in a "back to back" manner as compared with the "face to face" orientation in the Z crystals. Essentially, one hemidimer is rotated by ~70° and translated to the opposite side of the other hemidimer. This dramatically different conformation is accommodated by rearrangement of the linker.

While it is formally possible that the subunit orientation in the ΔZ structure represents a low activity conformation induced by the linker deletion, as compared with the high activity conformation of wild-type Z, this seems exceedingly unlikely. In the Z crystal structure, all four putative actin binding patches lie on the same surface of the dimer and could plausibly be accessible for interaction with actin. In contrast, in the ΔZ structure, the conserved surface surrounding Lys1601 is largely obscured in the interface between the hemidimers and could not interact with actin. How do both Z and ΔZ assemble actin despite the very different geometry of their putative actin binding surfaces? Flexibility in the linker provides an obvious solution to this conundrum. Based upon the fact that Z and ΔZ are both active in spite of their very different subunit orientations, and upon the considerable evidence for flexibility in the linker outlined above, we conclude that the FH2 domain is a flexibly tethered dimer.

The FH2 Domain Is Bivalent: Hemidimers Block Barbed End Elongation

Why must the FH2 domain dimerize in order to function properly? As described above, surface conservation and our mutagenesis studies show that the lasso/post interface is one likely site of interaction with actin. Thus, dimerization may be required to form this composite actin binding surface. Second, the FH2 domain may need to be "bivalent" in order to bind and/or assemble actin—that is, it may require *two* actin binding heads rather than one. Alternatively, it is possible that the intact FH2 dimer comprises a *single* actin binding head. Our previous studies of monomeric FH2 construct T (termed construct FH2Δ in Moseley et al., 2003) does not allow

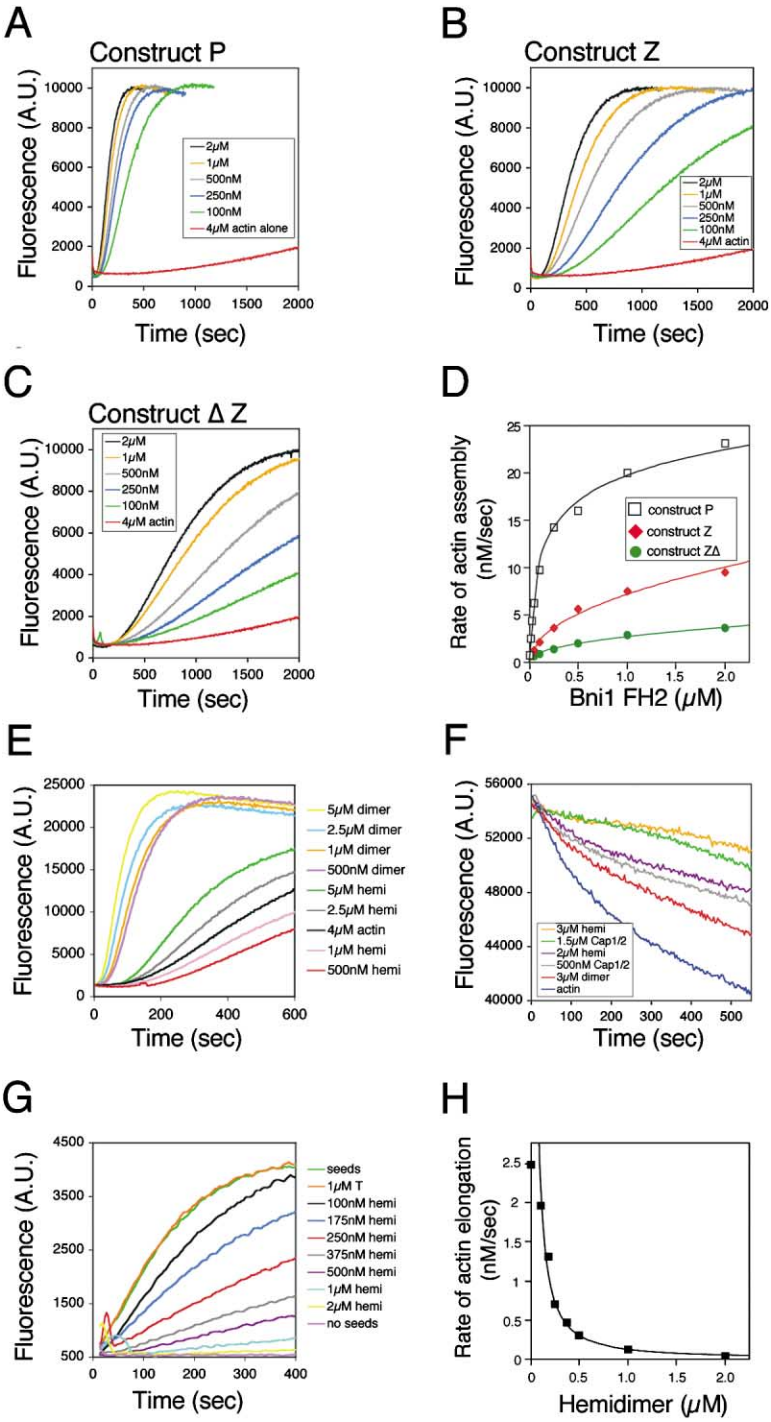

Figure 6. Actin Assembly and Elongation Activities of Bni1p FH2 Dimers and Hemidimers

(A–D) Effects on the rate of actin assembly kinetics of Bni1 constructs P (panel A), Z (panel B), and ΔZ (panel C) at a range of concentrations (100 nM to 2 μM). In (D), the rate of assembly during the early phase of actin polymerization is plotted for each construct as a function of FH2 construct concentration. Although these constructs show nanomolar potency in actin assembly (~200 nM for construct Z), they appear to be relatively inefficient nucleators. For example, we calculate that with 250 nM construct Z, the concentration of barbed ends is approximately 0.28 nM, or approximately 2 new barbed ends per thousand Z dimers (calculation assumes that the presence of the formin slows the rate of elongation by 50%). Other formin constructs appear to nucleate more efficiently (Li and Higgs, 2003; Moseley et al., 2003; Zigmond et al., 2003).

(E) Effects of hemidimer and uncleaved thrombin-Z dimer on actin assembly kinetics.

(F) Effects of hemidimer and uncleaved thrombin-Z dimer on the rate of disassembly of pre-formed actin filaments. Ten micromolar filamentous actin was diluted to 0.5 μM in the presence of the indicated concentrations of hemidimer, uncleaved thrombin-Z dimer, or yeast capping protein.

(G and H) Effects of hemidimer and construct T on the rate of elongation at the barbed ends of pre-existing filaments. Monomeric actin (0.5 μM, 10% pyrene-labeled) was polymerized at the barbed ends of mechanically sheared actin filament seeds (333 nM) in the presence of the indicated concentrations of hemidimer. In (H), the rates of filament elongation are plotted as a function of hemidimer concentration; rates were calculated from (G) as in Moseley et al. (2003).

us to discriminate between these possibilities because this construct lacks an intact lasso/post interface. In order to further dissect the role of dimerization, we sought to prepare and characterize hemidimers.

Based on the structure, we hypothesized that proteolytic cleavage in the linker segments would yield hemidimers; i.e., the knob-coiled-coil-post fragment of one subunit stably complexed with the cleaved lasso-linker fragment derived from the second subunit. Although trypsin and chymotrypsin readily cleave the FH2 domain within the linker, both also cleave at additional sites upon extended incubation or at higher stoichiometries (Supplemental Figure S4A online). Therefore, to facilitate purification of homogeneous hemidimers, we engineered a thrombin cleavage site in the linker. Comparison of the uncleaved thrombin-Z construct with wild-type Z revealed indistinguishable activity in an actin assembly assay (Figure 6E and data not shown). Furthermore, this construct forms dimers as expected (Supplemental Figure S4B). SDS-PAGE analysis of the thrombin-

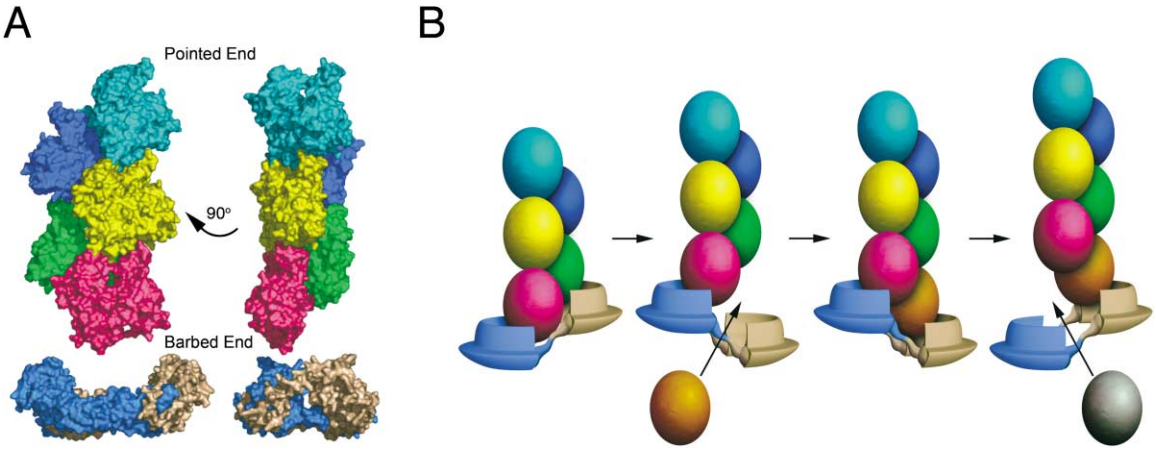

Figure 7. A Speculative Model Showing How the Tethered Dimer Architecture of the FH2 Domain Could Allow Stair-Stepping on the Elongating Barbed End of F-Actin

(A) Orthogonal views of the FH2 dimer positioned below the barbed end of a five-subunit actin filament. The FH2 domain is shown with one subunit colored blue and the other tan and is oriented so that the conserved top surface faces the barbed end of the filament.

(B) Schematic illustration showing how the FH2 domain might stair-step on the barbed end. Actin subunits are represented by colored ovals; the two halves of the formin dimer are colored as in (A). Alternating dissociation, displacement, and rebinding of one half of the formin dimer could allow elongation by addition of actin monomers to the barbed end of the filament.

Z protein after digestion with thrombin revealed two bands that migrated with the apparent molecular weights expected for the lasso-linker and knob-coiled-coil-post fragments (Supplemental Figure S4B). These two polypeptides copurified through consecutive anion-exchange and gel-filtration chromatography, indicating that they are stably associated as predicted. Furthermore, the complex eluted from the gel-filtration column at the volume expected for a ~48 kDa protein, confirming that the two hemidimers do indeed dissociate upon cleavage of the linker (Supplemental Figure S4B).

While the uncleaved thrombin-Z construct exhibits actin assembly activity characteristic of wild-type Z, the hemidimer is defective in actin assembly (Figure 6E). At concentrations at or below 1 μm, hemidimer decreases the rate of actin assembly as compared with that observed for actin alone. At very high concentrations of hemidimer (2.5 and 5 μm), a modest increase in assembly is observed. The assembly reactions carried out in the presence of hemidimer proceed with markedly different kinetics than the dimer-nucleated reactions, and they plateau at a lower level. These features could be explained by inhibition of barbed end elongation, together with weak nucleation and ensuing elongation from the pointed end, and would be expected of a barbed end capping protein. Thus we further characterized hemidimers by testing their activity in barbed end capping assays.

Capping proteins inhibit both assembly and disassembly of actin filaments. As shown in Figure 6G, hemidimers inhibit elongation from preformed actin seeds. Micromolar concentrations of hemidimer completely block elongation, and half-maximal inhibition of elongation is achieved with concentrations of approximately 175 nM hemidimer (Figure 6H). In contrast, the uncleaved thrombin-Z dimer acts as a processive cap as expected, only modestly slowing elongation and protecting growing barbed ends from high concentrations of capping protein (Supplemental Figure S6). Construct T (the monomeric knob-coiled-coil-post construct in which the lasso is deleted) shows no inhibition of assembly with concentrations up to 1 μM (Figure 6G). The lack of activity of T, as compared with the potent inhibition observed with the hemidimer, shows that an intact lasso/post interface is required for interaction with actin. Inhibition of elongation by hemidimer must stem from barbed end binding, rather than sequestration of actin monomers, because hemidimers also inhibit disassembly of actin filaments (Figure 6F). Additionally, we find no evidence that hemidimer can bind actin monomers in native-PAGE or nucleotide exchange assays (data not shown). In summary, these experiments show that (1) the hemidimer is competent to bind actin filaments but it completely blocks elongation, rather than acting as a processive cap, (2) the lasso is required in trans (from the opposite subunit in the dimer) to complete the actin binding surface of each hemidimer, (3) normal nucleation and processive capping require the intact FH2 dimer. Thus, from a functional perspective, the FH2 "tethered dimer" architecture consists of two actin binding heads connected by flexible linkers at either end. While one head (hemidimer) is sufficient to bind F-actin, the nucleation and processive capping activities of the formin depend upon the stable connection of the two binding heads in the tethered dimer.

Mechanistic Implications of the Tethered Dimer

Note that the function of the FH2 domain as a processive cap is not yet rigorously established and thus remains a working model. Experiments showing that FH2 domains protect elongating barbed ends from heterodimeric capping protein and partially, but not completely, cap the barbed end support this hypothesis, but more conclusive tests are needed. Nevertheless, it is important to consider how the structure of the FH2 domain might relate to this hypothesized function, and how the struc-

ture can facilitate further biophysical and biochemical investigations of FH2 function.

The dimensions of the FH2 domain are appropriate for interaction with the barbed end (Figure 7A). The two actin subunits at the barbed end of F-actin are related by pseudo 2_1 helical symmetry; they are related by a rotation of 166° and a translation of 27.5 Å along the filament axis (Lorenz et al., 1993). As demonstrated above, each half of the dimer is expected to be competent to bind actin. The antiparallel orientation of the two binding heads, together with sufficient flexibility between them, could allow each to make similar interactions at the barbed end. Modeling of the FH2 structure on the barbed end of the actin filament demonstrates that the 17 residue linker, if flexible, could provide a tether of sufficient length to span the 27.5 Å offset and allow the two sides of the FH2 dimer to interact in a similar manner with the two subunits at the barbed end of F-actin (data not shown). Furthermore, the tethered dimer architecture of the FH2 domain could allow formins to maintain a stable association with the elongating barbed end of a filament (Figure 7B). One side of the FH2 dimer could dissociate to promote incorporation of an additional actin monomer while the other side remained bound. Alternating dissociation of each half of the FH2 dimer, in a "stair stepping" fashion, would thereby allow the formin molecule to processively "ride" the elongating barbed end of an actin filament.

The stair-stepping mechanism implies anticooperativity in the two actin binding heads; i.e., relatively high affinity binding of one head and weak binding of the second head, with these affinities rapidly reversed upon incorporation of an additional actin subunit. From a structural perspective, anticooperativity would not be surprising because the two subunits at the barbed end (one protruding and one recessed) have very different local environments and could differ significantly in conformation and/or steric availability to bind to the FH2 domain. Furthermore, these environments "switch" upon incorporation of an additional subunit (See Figure 7A, addition of an actin subunit at the barbed end makes the magenta subunit precisely equivalent to the green subunit prior to the addition. Similarly, the newly added subunit is equivalent to the magenta subunit before addition). Because the presence of a formin dimer only modestly slows filament elongation or depolymerization in vitro (Pruyne et al., 2002; Sagot et al., 2002b; Moseley et al., 2003; Pring et al., 2003; Li and Higgs, 2003), the "weak" side must have a rapid off rate and any conformational rearrangements must occur on the same time scale as monomer addition. We have not explicitly measured the affinity of the Bni1p hemidimer for actin filaments, but we observe half-maximal inhibition of elongation with ~200 nM hemidimer. The intact dimer is reported to bind the barbed end with an apparent k_d of 7–20 nM (Moseley et al., 2003; Pring et al., 2003), one or two orders of magnitude more tightly than hemidimer. Therefore, if the affinity we observe with the hemidimer is representative of the high affinity "strong" side of the dimer, then the "weak" side of the dimer would only need to bind with a k_d = ~10 mM to produce the low nanomolar affinity observed for the intact dimer (assuming simple additive affinities of the two sides of the dimer, $k_d = [200 \times 10^{-9}][10 \times 10^{-3}]M = 2$ nM). This low affinity is consistent with the requirement for rapid dissociation of the weak binding head in order to allow monomer addition at a rate of >100 monomers/s as observed for elongation of actin cables in yeast (Yang and Pon, 2002).

The mode of formin interaction with actin during nucleation might or might not be equivalent to its mode of interaction during elongation. The inherently bivalent FH2 dimer could promote nucleation by stabilizing a two-protomer nucleus for actin polymerization. This could occur with each hemidimer contacting primarily one actin subunit, or with one or both bridging between actin subunits. The fact that hemidimers and intact dimers bind filament ends with considerably higher affinity than G-actin suggests that they must either recognize a site within an actin subunit that is unique to the F-actin conformation or recognize an epitope that spans between subunits (or both). Thus, binding of hemidimers would be expected to stabilize an F-actin conformation and to at least weakly promote nucleation. Our observation that the intact dimer is at least two orders of magnitude more potent than the hemidimer in nucleation assays indicates that the integrity of the tethered dimer is also critical for proper nucleation activity.

The suitability of the tethered dimer architecture for the proposed role of formins is striking. It appears to be precisely that required for the stair-stepping mechanism suggested by recent biochemical observations that formins persistently cap the barbed end of growing actin filaments (Moseley et al., 2003; Zigmond et al., 2003). Our structural and biochemical data provide compelling evidence that the relative orientation of the two hemidimers is not rigidly defined; i.e., that the FH2 domain is a flexibly tethered dimer. However, they do not explicitly address the question of whether this flexibility is *required* for function, nor whether it serves to allow the dimer to span the offset at the barbed end as we hypothesize (Figure 7B). The structure will stimulate further experiments that address these and other mechanistic questions.

Experimental Procedures

Protein Expression, Purification, and Crystallization

Construct Z (residues 1348–1766 of the Bni1p FH2 domain) was expressed as a Glutathione S-transferase fusion with a tobacco etch virus (TEV) protease site. The fusion protein was purified on Glutathione Sepharose 4B, eluted with free glutathione, cleaved with TEV protease, and the free FH2 domain was further purified by Mono-Q anion exchange chromatography. The protein was maintained in storage buffer containing 200 mM NaCl and 20 mM Hepes, pH 7.5. Point mutations studied here were introduced using the Quikchange procedure (Stratagene). Construct P was also expressed as a GST-fusion with a TEV cleavage site, but the cleaved protein includes residues 1348–1750 of Bni1p plus a C-terminal 6-His tag. Construct ΔZ was identical to Z, except that residues 1411–1416 were deleted and replaced with two residues (Glu-Phe) introduced by the mutagenesis procedure. Both P and ΔZ proteins were purified as described for Z. Further details are included in the Supplemental Data.

For crystallization, the Z protein was concentrated to 8 mg/ml in storage buffer and p-chloromercuribenzenesulfonic acid (PCMBS) was added to 2.5 mM. Crystals were obtained at 20°C in hanging drops using 16% ethylene glycol as a precipitant. The crystals belong to hexagonal space group $P6_122$ with unit cell dimensions of a = b = 101.4 Å, c = 265.7 Å. The asymmetric unit contains a single FH2 polypeptide chain. The ΔZ protein was crystallized in hanging

drops by vapor diffusion against 0.8 M sodium potassium phosphate, 100 mM HEPES pH 7.5, and 30% glycerol. The crystals belong to space group C2 with unit cell dimensions a = 98 Å, b = 172.2 Å, c = 120.6 Å, and β = 112.3°,and contain two subunits per asymmetric unit.

Structure Determination and Refinement

Detailed crystallographic methods are presented in the supplementary materials. Briefly, for the construct Z, crystals diffraction data were collected at the Cornell High Energy Synchrotron Source (CHESS) at 100 K, and the structure was determined by MAD phasing using data recorded from PCMBS-derivatized crystals and from crystals that were both PCMBS-derivatized and selenomethionine-substituted (Table 1). The electron density map was improved with solvent flattening in CNS (Brunger et al., 1998); the resulting map allowed construction of an essentially complete atomic model with the program O (Jones and Kjeldgaard, 1997). Due to the marked anisotropy of diffraction, further refinement with CNS was performed using a data set truncated to include only the reflections contained within an ellipsoid of revolution with axes corresponding to the observed diffraction limits in the c* and a* directions (2.5 and 3.1 Å, respectively). The final model contains 411 continuous amino acids, 1 PCMBS molecule, 1 mercury atom, and 30 water molecules and has been refined to an R value of 20.7% (R_{free} = 25.1%).

For the ΔZ crystals, X-ray diffraction data were collected on NE-CAT beamline 8-BM at the Advanced Photon Source (Table 1). The structure was determined by molecular replacement using the Z hemidimer as a search model. After an initial round of refinement with CNS, electron density maps showed density for the linkers, which were not included in the initial model, allowing unambiguous assignment of the dimer organization. The linkers were constructed and the structure was refit and further refined to a crystallographic R value of 23.4% (R_{free} = 28.8%) at 3.3 Å resolution.

Preparation of Hemidimers

The thrombin-Z construct was prepared by replacing the wild-type Arg1402 codon (*agg*) with a different Arg codon (*cga*) to introduce a unique XhoI site. A synthetic linker encoding the sequence **REI KSL**VPR'**GSGSLQ** (native sequence in bold, thrombin recognition site underlined, thrombin cleavage site indicated by ') was then ligated into construct Z using this XhoI site and a unique PstI site 42 bases downstream. The thrombin-Z dimer was purified as previously described for construct Z, then hemidimer was produced by overnight digestion with thrombin, followed by further purification by anion-exchange and gel-filtration chromatography.

Actin Assembly Assays

For actin assembly, filament elongation, and filament depolymerization reactions, rabbit skeletal muscle actin was purified as described (Spudich and Watt, 1971) and labeled with pyrenyliodoacetamide (Higgs et al., 1999; Pollard, 1984). Actin monomers were prepared by gel filtration using a Sephacryl S-200 column equilibrated in G-buffer (10 mM Tris [pH 8.0], 0.2 mM ATP, 0.2 mM $CaCl_2$, and 0.2 mM DTT). Actin filament assembly assays were performed as previously described (Humphries et al., 2002). Briefly, gel filtered monomeric actin (final concentration 2 or 4 μM, 5% pyrene-labeled) was mixed with 15 μl HEK buffer (20 mM Hepes [pH 7.4], 1 mM EDTA, 50 mM KCl) or proteins in HEK buffer, and this mixture was added immediately to 3 μl of 20× initiation mix (40 mM $MgCl_2$, 10 mM ATP, 1 M KCl) to initiate actin assembly. Pyrene fluorescence was monitored at excitation 365 nm and emission 407 nm in a fluorescence spectrophotometer (Photon Technology International, Lawrenceville, New Jersey) held at 25°C. Rates of actin assembly were calculated from the maximal slopes of assembly curves, obtained in the first half of reactions. Filament elongation assays were performed as described (Moseley et al., 2003). For filament depolymerization assays, a 10 μM stock of F-actin (50% pyrene-labeled) was diluted to 0.5 μM (100 μl final volume) in the presence of F buffer (G buffer supplemented with 1× initiation mix) and 10 μl HEK buffer or proteins in HEK buffer. Pyrene fluorescence was monitored as above.

Acknowledgments

We thank Q. Hao at CHESS, C. Ogata at NE-CAT, and T. Boggon for help with synchrotron data collection. We thank Sally Zigmond for helpful discussions and Y. Li for assistance with protein purification and crystallization. M.J.E. and D.P. are Scholars of the Leukemia and Lymphoma Society. B.L.G. was supported by a Pew Scholars award. This work was supported in part by NIH proposals GM61345 (D.P.) and GM63691 (B.L.G.).

Received: December 15, 2003
Revised: January 12, 2004
Accepted: February 18, 2004
Published: March 4, 2004

References

Alberts, A.S. (2001). Identification of a carboxyl-terminal diaphanous-related formin homology protein autoregulatory domain. J. Biol. Chem. *276*, 2824–2830.

Bateman, A., Birney, E., Cerruti, L., Durbin, R., Etwiller, L., Eddy, S.R., Griffiths-Jones, S., Howe, K.L., Marshall, M., and Sonnhammer, E.L. (2002). The Pfam protein families database. Nucleic Acids Res. *30*, 276–280.

Brunger, A.T., Adams, P.D., Clore, G.M., DeLano, W.L., Gros, P., Grosse-Kunstleve, R.W., Jiang, J.S., Kuszewski, J., Nilges, M., Pannu, N.S., et al. (1998). Crystallography & NMR system: A new software suite for macromolecular structure determination. Acta Crystallogr. D Biol. Crystallogr. *54*, 905–921.

Castrillon, D.H., and Wasserman, S.A. (1994). Diaphanous is required for cytokinesis in Drosophila and shares domains of similarity with the products of the limb deformity gene. Development *120*, 3367–3377.

Evangelista, M., Blundell, K., Longtine, M.S., Chow, C.J., Adames, N., Pringle, J.R., Peter, M., and Boone, C. (1997). Bni1p, a yeast formin linking cdc42p and the actin cytoskeleton during polarized morphogenesis. Science *276*, 118–122.

Evangelista, M., Pruyne, D., Amberg, D.C., Boone, C., and Bretscher, A. (2002). Formins direct Arp2/3-independent actin filament assembly to polarize cell growth in yeast. Nat. Cell Biol. *4*, 260–269.

Evangelista, M., Zigmond, S., and Boone, C. (2003). Formins: signaling effectors for assembly and polarization of actin filaments. J. Cell Sci. *116*, 2603–2611.

Feierbach, B., and Chang, F. (2001). Roles of the fission yeast formin for3p in cell polarity, actin cable formation and symmetric cell division. Curr. Biol. *11*, 1656–1665.

Higgs, H.N., Blanchoin, L., and Pollard, T.D. (1999). Influence of the C terminus of Wiskott-Aldrich syndrome protein (WASp) and the Arp2/3 complex on actin polymerization. Biochemistry *38*, 15212–15222.

Humphries, C.L., Balcer, H.I., D'Agostino, J.L., Winsor, B., Drubin, D.G., Barnes, G., Andrews, B.J., and Goode, B.L. (2002). Direct regulation of Arp2/3 complex activity and function by the actin binding protein coronin. J. Cell Biol. *159*, 993–1004.

Imamura, H., Tanaka, K., Hihara, T., Umikawa, M., Kamei, T., Takahashi, K., Sasaki, T., and Takai, Y. (1997). Bni1p and Bnr1p: downstream targets of the Rho family small G-proteins which interact with profilin and regulate actin cytoskeleton in Saccharomyces cerevisiae. EMBO J. *16*, 2745–2755.

Jones, T.A., and Kjeldgaard, M. (1997). Electron-density map interpretation. Methods Enzymol. *277*, 173–208.

Kaksonen, M., Sun, Y., and Drubin, D.G. (2003). A pathway for association of receptors, adaptors, and actin during endocytic internalization. Cell *115*, 475–487.

Kohno, H., Tanaka, K., Mino, A., Umikawa, M., Imamura, H., Fujiwara, T., Fujita, Y., Hotta, K., Qadota, H., Watanabe, T., et al. (1996). Bni1p implicated in cytoskeletal control is a putative target of Rho1p small GTP binding protein in Saccharomyces cerevisiae. EMBO J. *15*, 6060–6068.

Kovar, D.R., Kuhn, J.R., Tichy, A.L., and Pollard, T.D. (2003). The

fission yeast cytokinesis formin Cdc12p is a barbed end actin filament capping protein gated by profilin. J. Cell Biol. *161*, 875–887.

Li, F., and Higgs, H.N. (2003). The Mouse formin mDia1 is a potent actin nucleation factor regulated by autoinhibition. Curr. Biol. *13*, 1335–1340.

Lorenz, M., Popp, D., and Holmes, K.C. (1993). Refinement of the F-actin model against X-ray fiber diffraction data by the use of a directed mutation algorithm. J. Mol. Biol. *234*, 826–836.

Moreau, V., Madania, A., Martin, R.P., and Winson, B. (1996). The Saccharomyces cerevisiae actin-related protein Arp2 is involved in the actin cytoskeleton. J. Cell Biol. *134*, 117–132.

Moseley, J.B., Sagot, I., Manning, A.L., Xu, Y., Eck, M.J., Pellman, D., and Goode, B.L. (2003). A conserved mechanism for Bni1- and mDia1-induced actin assembly and dual regulation of Bni1 by Bud6 and profilin. Mol. Biol. Cell. *15*, 896–907.

Petersen, J., Nielsen, O., Egel, R., and Hagan, I.M. (1998). FH3, a domain found in formins, targets the fission yeast formin Fus1 to the projection tip during conjugation. J. Cell Biol. *141*, 1217–1228.

Pollard, T.D. (1984). Polymerization of ADP-actin. J. Cell Biol. *99*, 769–777.

Pollard, T.D., Blanchoin, L., and Mullins, R.D. (2000). Molecular mechanisms controlling actin filament dynamics in nonmuscle cells. Annu. Rev. Biophys. Biomol. Struct. *29*, 545–576.

Pring, M., Evangelista, M., Boone, C., Yang, C., and Zigmond, S.H. (2003). Mechanism of formin-induced nucleation of actin filaments. Biochemistry *42*, 486–496.

Pruyne, D., Evangelista, M., Yang, C., Bi, E., Zigmond, S., Bretscher, A., and Boone, C. (2002). Role of formins in actin assembly: nucleation and barbed-end association. Science *297*, 612–615.

Pupko, T., Bell, R.E., Mayrose, I., Glaser, F., and Ben-Tal, N. (2002). Rate4Site: an algorithmic tool for the identification of functional regions in proteins by surface mapping of evolutionary determinants within their homologues. Bioinformatics *18* (*Suppl 1*), S71–S77.

Robinson, R.C., Turbedsky, K., Kaiser, D.A., Marchand, J.B., Higgs, H.N., Choe, S., and Pollard, T.D. (2001). Crystal structure of Arp2/3 complex. Science *294*, 1679–1684.

Sagot, I., Klee, S.K., and Pellman, D. (2002a). Yeast formins regulate cell polarity by controlling the assembly of actin cables. Nat. Cell Biol. *4*, 42–50.

Sagot, I., Rodal, A.A., Moseley, J., Goode, B.L., and Pellman, D. (2002b). An actin nucleation mechanism mediated by Bni1 and profilin. Nat. Cell Biol. *4*, 626–631.

Spudich, J.A., and Watt, S. (1971). The regulation of rabbit skeletal muscle contraction. I. Biochemical studies of the interaction of the tropomyosin-troponin complex with actin and the proteolytic fragments of myosin. J. Biol. Chem. *246*, 4866–4871.

Tominaga, T., Sahai, E., Chardin, P., McCormick, F., Courtneidge, S.A., and Alberts, A.S. (2000). Diaphanous-related formins bridge Rho GTPase and Src tyrosine kinase signaling. Mol. Cell *5*, 13–25.

Wallar, B.J., and Alberts, A.S. (2003). The formins: active scaffolds that remodel the cytoskeleton. Trends Cell Biol. *13*, 435–446.

Watanabe, N., Madaule, P., Reid, T., Ishizaki, T., Watanabe, G., Kakizuka, A., Saito, Y., Nakao, K., Jockusch, B.M., and Narumiya, S. (1997). p140mDia, a mammalian homolog of Drosophila diaphanous, is a target protein for Rho small GTPase and is a ligand for profilin. EMBO J. *16*, 3044–3056.

Watanabe, N., Kato, T., Fujita, A., Ishizaki, T., and Narumiya, S. (1999). Cooperation between mDia1 and ROCK in Rho-induced actin reorganization. Nat. Cell Biol. *1*, 136–143.

Winter, D., Podtelejnikov, A.V., Mann, M., and Li, R. (1997). The complex containing actin-related proteins Arp2 and Arp3 is required for the motility and integrity of yeast actin patches. Curr. Biol. *7*, 519–529.

Yang, H.C., and Pon, L.A. (2002). Actin cable dynamics in budding yeast. Proc. Natl. Acad. Sci. USA *99*, 751–756.

Zigmond, S.H., Evangelista, M., Boone, C., Yang, C., Dar, A.C., Sicheri, F., Forkey, J., and Pring, M. (2003). Formin leaky cap allows elongation in the presence of tight capping proteins. Curr. Biol. *13*, 1820–1823.

Accession Numbers

Atomic Coordinates have been deposited in the Protein Data Bank under accession codes 1UX5 (for the construct Z structure) and 1UX4 (for the delta-Z structure).